



Structural Properties of Fe Doped TiO₂ Nanorods Prepared by Low Cost Hydrothermal Method

Sattar J. Hashim ^{a*}, Khaleel I. Hassoon ^b, Odai N. Salman ^c

^a Department of Applied Sciences, University of Technology, Baghdad, Iraq, sattarjabir314@gmail.com

^b Department of Applied Sciences, University of Technology, Baghdad, Iraq, kihassoun@yahoo.com

^c Department of Applied Sciences, University of Technology, Baghdad, Iraq, micro_ud@yahoo.com

*Corresponding author.

Submitted: 16/08/2020

Accepted: 06/09/2020

Published: 25/12/2020

KEY WORDS

Fe-doped TiO₂, aligned nanorods and Hydrothermal method

ABSTRACT

In this work, titanium dioxide films were deposited on fluorine tin oxide (FTO)-glass substrates using Hydrothermal method. A low-cost homemade autoclave was used to fabricate pure TiO₂ and Fe-doped (0.1%, 0.3%, 0.5%, 0.7% and 1.5%) films. X-ray diffraction patterns showed that the predominant phase is rutile (R-TiO₂) with peaks at (101), (002) and (112). The Field Emission Scanning Electron Microscope (FESEM) top and cross-sectional images indicated that the films have vertically aligned nanorods structures with parallelogram cross-sectional areas and aspect ratio range (9.2-15.3).

How to cite this article: S. J. Hashim, K. I. Hassoon and O. N. Salman, "Structural Properties of Fe doped TiO₂ Nanorods Prepared by Low Cost Hydrothermal Method," Engineering and Technology Journal, Vol. 38, Part B, No. 03, pp.177-183, 2020.

DOI: <https://doi.org/10.30684/etj.v38i3B.1800>

This is an open access article under the CC BY 4.0 license <http://creativecommons.org/licenses/by/4.0>.

1. INTRODUCTION

In recent years, titanium dioxide thin and thick films have found many applications because of their chemical stability, non-toxicity and possession of unique optical characteristics; such as good photocatalytic activity, high melting point, and high reflective index wide direct-bandgap, which means high transmittance in the visible and near-IR regions. For example, in the last two decades, TiO₂ films have been used extensively as anode in dye sensitized solar cells [1], as a photocatalyst [2], an antireflection coating in silicon solar cells [3] and a gas sensor [4].

TiO₂ has been prepared using physical thermal vapor deposition [5], chemical bath deposition [6], chemical spray pyrolysis [7], hydrothermal method [8], etc.

Transition metals were used as dopants to enlarge the range of TiO_2 's spectral absorption to include the visible region. In that respect, iron is frequently utilized as dopant because its half-filled electronic configuration is compatible with Ti^{4+} . Consequently, Fe has the ability to narrow the energy gap via formation of new intermediate energy levels [9]. Therefore, Fe^{3+} dopants can substitute Ti^{4+} and form shallow charge traps within the TiO_2 . The doping with Fe^{3+} dopants reduces the electron-hole recombination and hence improves the properties for photovoltaic and photocatalytic applications [8, 11, 12].

TiO_2 as a bulk material has two main tetragonal phases, anatase system (A- TiO_2) and rutile system (R- TiO_2). The R- TiO_2 phase, which is formed at higher temperatures, has a refractive index $n=2.7$, while A- TiO_2 has a refractive index $n=2.5$ [12]. In general, the structure of TiO_2 films strongly depends on the preparation method, deposition temperature and substrate surface properties [8, 11, 13].

The aim of the present work is to study the possibility of growing TiO_2 nanorods using low cost hydrothermal method and the effect of Fe-doping on the structural properties of TiO_2 prepared by this technique.

2. EXPERIMENTAL DETAILS

In this work, FTO-glass slides (TEC 8 with 600 nm in thickness from DyeSol) were used as substrates. The substrates were ultrasonically cleaned for 15 minutes using acetone, ethanol, and double distilled water (purchased from a local store). Then, the samples were dried in air and placed at angle 45° inside a sealed container made of Teflon. A volume of HCl acid (37% Sigma-Aldrich) was dissolved in 20 mL of double distilled water and thoroughly mixed using magnetic stirrer for 5 min. After that, (1.017-1.033 mL) of titanium butoxide (Sigma-Aldrich) was blended with the solution and kept for another 5 min. The doping of TiO_2 was implemented by adding $\text{Fe}(\text{NO}_3)_3 \cdot 9\text{H}_2\text{O}$ (from HiMedia Laboratories Pvt. Ltd) as a precursor of Fe to maintain the atomic ratio of Fe/Ti (0%, 0.1%, 0.3%, 0.7% and 1.5%). The solution was stirred again for 90 min. At first, the mixture was clear and transparent but after adding the Iron nitrate nonahydrate it became near to Green. 20 mL of the mixture is charged to homemade stainless steel autoclave (30 mL). The autoclave was put inside an electric oven. The oven was preheated at 180°C (± 3 ramp rate) for three hours. After this time, the autoclave was removed out of the oven and slowly cooled down under stream of water and the FTO glass substrate brought out and rinsed with distilled water many times to remove any extra reactants, finally the samples were dried in air at RT for 15 min. The prepared samples were characterized by XRD of Cu $K\alpha$ ($\lambda=1.5405 \text{ \AA}$) with scan rate 8 (deg/min), and the scanning range was 20 to 75° in step-size 0.02° . The x-ray voltage was 40 kV, and the current was 30 mA (College of Education Ibn al-Haytham). The FESEM, which is supported with Energy Dispersive Spectroscopy (EDS), was used to view the TiO_2 nanorods (Razi Applied Science Foundation - Tehran, Iran).

3. RESULTS AND DISCUSSION

Figure 1 reveals the diffractograms of XRD for TiO_2 nanorods with different Fe concentrations (0, 0.1, 0.3, 0.5, 0.7 and 1.5 at. %). The peaks in XRD patterns belong to tetragonal rutile titanium dioxide (R- TiO_2). The location of these peaks agree well with (JCPDS 89-4920 card). No other peaks related to the different phases of TiO_2 have been identified. As seen in the figure, the stars represent the diffraction peaks for FTO substrate, and R represents the Rutile phase of TiO_2 . Moreover, no peak belongs to Fe is observed in the diffraction patterns and this confirms that no agglomeration of iron atoms is found. The highest three diffraction peaks of TiO_2 are $2\theta = (35.946^\circ, 62.673^\circ, \text{ and } 69.681^\circ)$ which are corresponding to the planes (101), (002) and (112), respectively. The results manifested that the as-deposited TiO_2 films have the highest intensity peaks at $2\theta=62.673^\circ$ (002). Furthermore, there is a slight reduction in some peaks and this reduction is also reported by L. Wan [14]. Also, there is a slight displacement of the (101) and (002) planes toward the right side, while the (112) is shifted toward the left side of the 2θ axis. This behavior is constant even at the high doping concentrations of Fe, as shown in Table (1). It is worthwhile to mention that the main reason that makes the hydrothermal method produce R phase rather than the other phase of TiO_2 is that FTO and R- TiO_2 have a low mismatch parameter [15].

In order to calculate the X-Ray parameters, the following equations [16] are used, and the results are presented in Table (1):

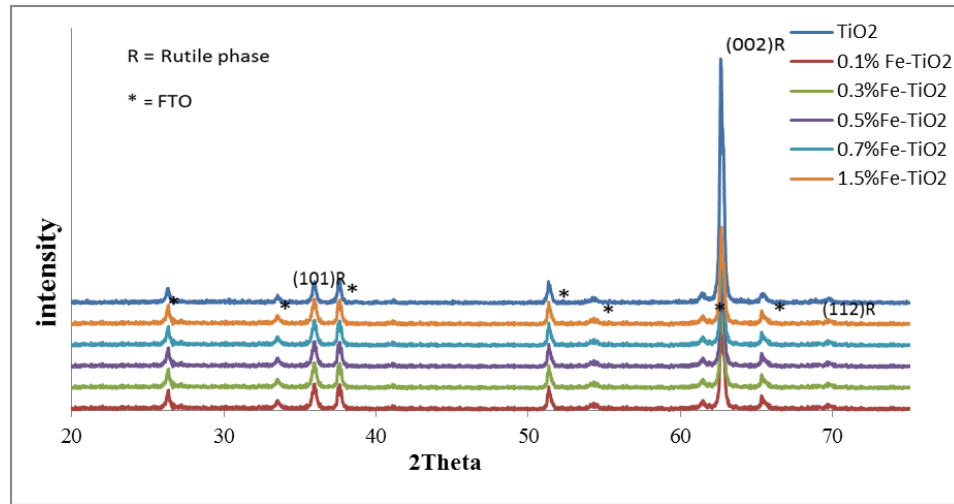


Figure 1: XRD-diffractograms for the R-TiO₂ samples with different doping concentrations of Fe on the FTO-glass by the hydrothermal technique.

TABLE I: The effect of Fe concentrations on the XRD parameters for TiO₂.

Sample	2 θ (deg)	hkl	d-spacing (Å)	FWHM β (rad)	D (nm)	(S) *10 ⁻³ (lines/nm ²)	ϵ *10 ⁻³
TiO ₂	35.9450	101	2.49643	0.29600	28.2396	0.00125	0.41
	62.6772	002	1.48108	0.23380	39.8151	0.00063	0.62
	69.72	112	0.13480	0.29330	33.0441	0.00091	0.89
0.1%Fe-TiO ₂	35.9527	101	2.49591	0.34000	24.5845	0.00165	0.48
	62.6968	002	1.48066	0.22890	40.6717	0.00060	0.60
	69.6747	112	1.34845	0.29330	33.0269	0.00091	0.89
0.3%Fe-TiO ₂	35.9527	101	2.49591	0.34000	24.5845	0.00165	0.48
	62.6968	002	1.48066	0.22890	40.6717	0.00060	0.60
	69.6747	112	1.34845	0.29330	33.0269	0.00091	0.89
0.5%Fe-TiO ₂	35.9527	101	2.49591	0.34000	24.5845	0.00165	0.48
	62.6968	002	1.48066	0.22890	40.6717	0.00060	0.60
	69.6747	112	1.34845	0.29330	33.0269	0.00091	0.89
0.7%Fe-TiO ₂	35.9527	101	2.49591	0.34000	24.5845	0.00165	0.48
	62.6968	002	1.48066	0.22890	40.6717	0.00060	0.60
	69.6747	112	1.34845	0.29330	33.0269	0.00091	0.89
1.5%Fe-TiO ₂	35.9527	101	2.49591	0.34000	24.5845	0.00165	0.48
	62.6968	002	1.48066	0.22890	40.6717	0.00060	0.60
	69.6747	112	1.34845	0.29330	33.0269	0.00091	0.89

$$D = \frac{\kappa\lambda}{\beta(\cos\theta)} \quad (1)$$

$$S = \frac{1}{D^2} \quad (2)$$

$$\varepsilon = \frac{\beta}{4 \tan \theta} \quad (3)$$

Where, D is the crystallite size, λ is the x-ray wavelength, β is the full-width at half-maximum intensity (FWHM), δ is the density of dislocation defects, ε is the strain, θ represents the Bragg's diffraction angle, and K is a constant value. S. Manu et al. [17] investigated the effect of iron-doping on the structure properties of the TiO_2 . The authors reported that there was no effect of the Fe ions when the ions percentage was (0-2%) as in the present case.

Figures 2 and 3 depict the top and cross-sectional views of TiO_2 films synthesized at 180°C for 3 h for different doping concentrations of Fe. The images reveal that the TiO_2 films deposited on the FTO substrate are vertically aligned nanorods. Identical structures of nanorods have been also reported in Liu and Aydil [18]. The nanorods are very dense and almost vertically grown on the FTO substrate. The nanorods have square cross-sectional ends ranging from (50-300 nm) in diameter, and the rod lengths are about ($4.6 \mu\text{m}$), so that the aspect ratio can be estimated to be about (9.2-15.3), which is defined as the ratio of the length of the nanorod to its diameter. Furthermore, it can be seen from the top and side views of Figure 2 that the nanorods are attached together from the bottom while, they detached at the surface. In general, no clear effect of Fe-doping on the structural properties of TiO_2 nanorods.

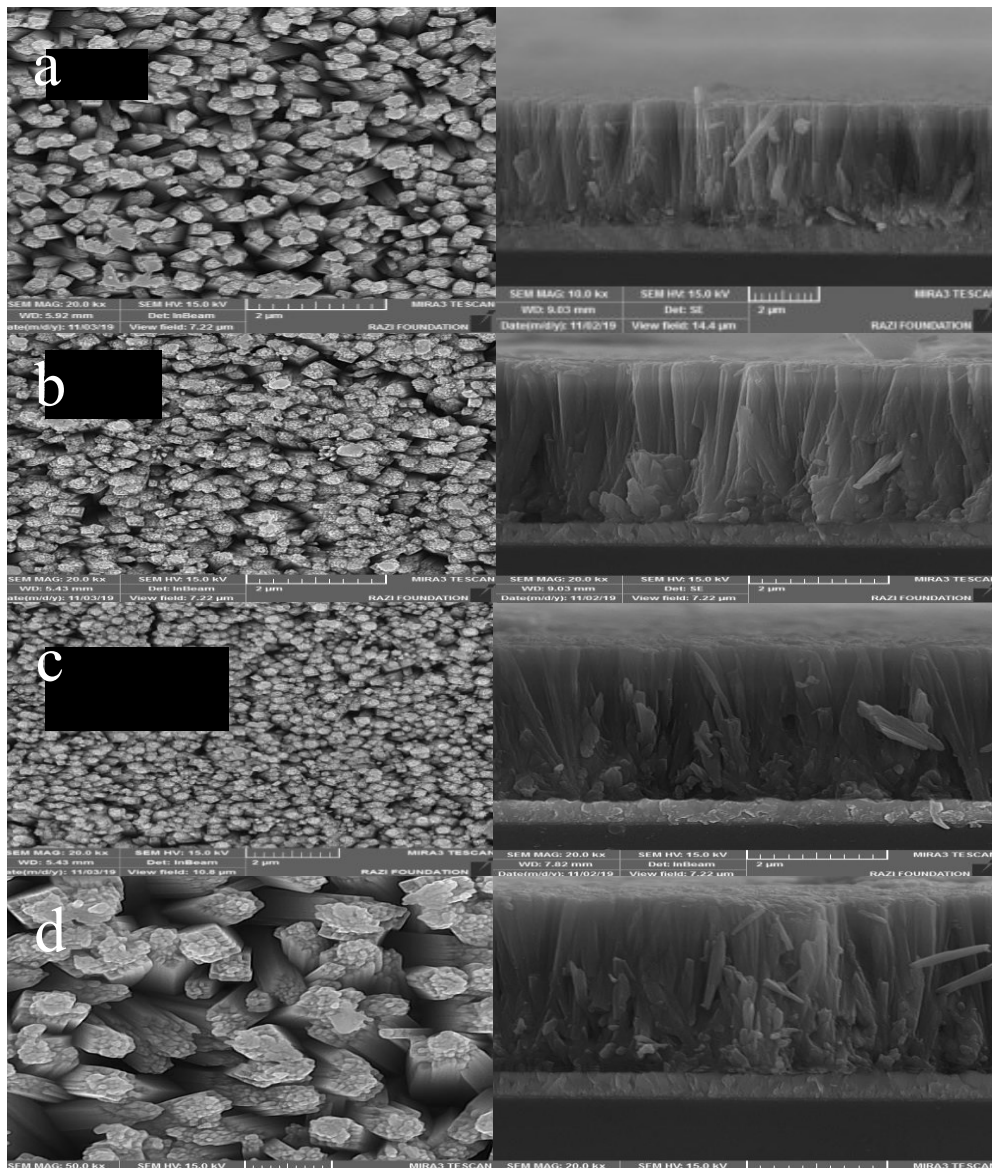


Figure 2: Images of FESEM of top with its side view for the samples (a) TiO_2 , (b) 0.1% Fe- TiO_2 , (c) 0.3% Fe- TiO_2 , and (d) 0.5% Fe- TiO_2 .

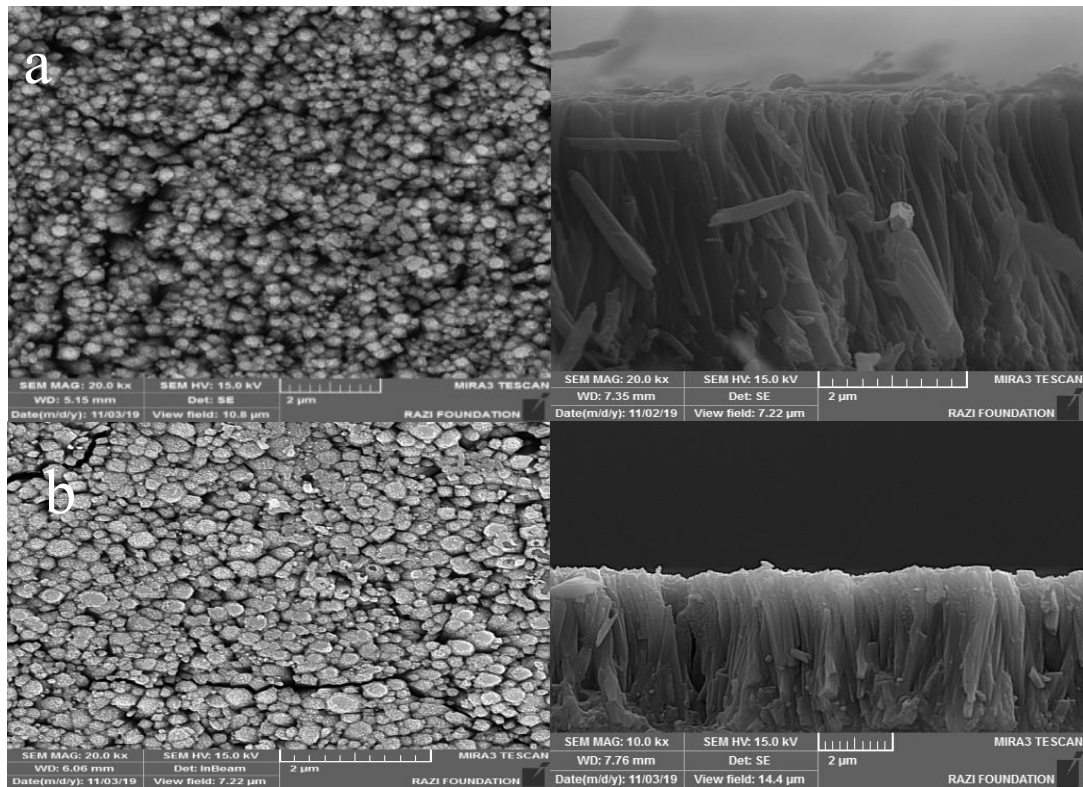


Figure 3: Pictures of FESEM, top with its cross section at right of (a) 0.7% Fe-TiO₂ and (b) 1.5% Fe-TiO₂.

The energy dispersive x-ray diffraction spectroscopy (EDS) was utilized here to identify the elemental composition of TiO₂ films for pure and doped TiO₂. Figure 4, confirms that the major constituents of the nanorods films are Titanium (Ti) and Oxygen (O). The peak of the (Au) is due to a gold layer deliberately deposited to increase the resolution of the FESEM images. Table (2) illustrates the actual atomic ratios of oxygen and Titanium in columns 1 and 2, respectively which resulted from the EDS device, the Ti/O ratio in column 3 is resulted by dividing column 1 on 2, and the stoichiometric ratio in column 4 represents the ratio of the reactants theoretically to the ratio practically extracted. From the results of Table (2), it is clear that the sample TiO₂ prepared by hydrothermal method has stoichiometric ratio 1:2 (i.e. TiO₂). Figure 4 demonstrates the EDS spectrum of (a), (b), (c) and (d) for the samples TiO₂, 0.1%Fe-TiO₂, 0.7% Fe-TiO₂, and 1.5% Fe-TiO₂, respectively.

TABLE II: The results of the EDX showing the proportion of elements in the films.

Samples	O (Atomic %)	Ti (Atomic %)	Ti/O Ratio	Stoichiometry Ratio %
TiO ₂	66.86	33.14	2.01	99.50
0.1%Fe-TiO ₂	72.3	27.7	2.61	76.62
0.7%Fe-TiO ₂	70.82	29.18	2.42	82.64
1.5%Fe-TiO ₂	69.28	30.72	2.25	88.88

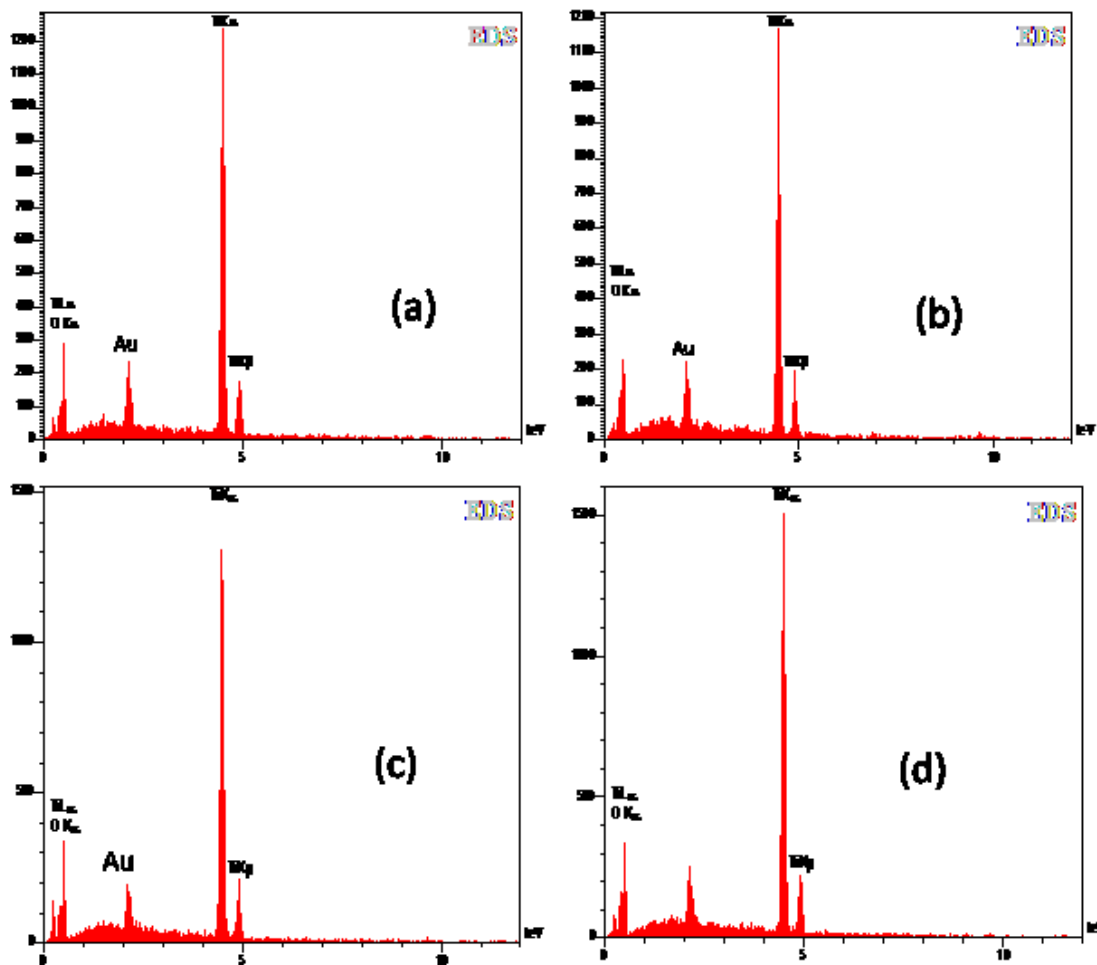


Figure 4: The EDS spectrum of (a), (b), (c) and (d) corresponding to the samples of pure TiO_2 , 0.1%Fe- TiO_2 , 0.7% Fe- TiO_2 and 1.5% Fe- TiO_2 , respectively.

4. CONCLUSIONS

TiO_2 nanorods with rutile structure can be prepared using simple hydrothermal technique. In conclusion, the doping of TiO_2 with Fe did not apparently change the crystalline structure of R- TiO_2 . However, the optical properties measurements revealed a slight reduction in the bandgap energy for the samples doped with Fe concentration (0.1, 0.3 and 0.5 %).

REFERENCES

- [1] B. Hu, Q. Tang, B. He, L. Lin and H. Chen, "Mesoporous TiO_2 anodes for efficient dye-sensitized solar cells: An efficiency of 9.86% under one sun illumination," *Journal of Power Sources*, vol. 267, pp.445-451, 2014.
- [2] T. Ohno, T. Mitsui, and M. Matsumura, "Photocatalytic Activity of S-doped TiO_2 Photocatalyst under Visible Light," *Journal of Chemistry Letters*, vol. 32, no.4, pp.364-365, 2003.
- [3] J. Szlufcik, J. Majewski, A. Buczkowski, J. Radojewski, L. Jędral, and E. B. Radojewska, "Screen-printed titanium dioxide anti-reflection coating for silicon solar cells," *Solar Energy Materials*, vol.18, no.5, pp.241–252, 1989.
- [4] B. Karunakaran, P. Uthirakumar, S. J. Chung, S. Velumani, and E.-K. Suh, " TiO_2 thin film gas sensor for monitoring ammonia," *Materials Characterization*, vol. 58, no.8-9, pp.680–684, 2007.
- [5] J. M. Wu, H. C. Shih, and W. T. Wu, "Formation and photoluminescence of single-crystalline rutile TiO_2 nanowires synthesized by thermal evaporation," *Nanotechnology*, vol.17, no.1, pp.105–109, 2005.
- [6] A. H. Mayabadi, V. S. Waman, M. M. Kamble, S. S. Ghosh, B. B. Gabhale, S. R. Rondiya, and A. V. Rokade, "Evolution of structural and optical properties of rutile TiO_2 thin films synthesized at room

- temperature by chemical bath deposition method,” *Journal of Physics and Chemistry of Solids*, vol.75, no.2, pp.182-187, 2014.
- [7] R. Ayouchi, C. Casteleiro, R. Schwarz, J. R. Barrado, and F. Martín, “Optical properties of TiO₂ thin films prepared by chemical spray pyrolysis from aqueous solutions,” *Physica Status Solidi C*, vol.7, no.3-4, pp.933-936, 2010.
- [8] Q. Chen, Y. Qian, Z. Chen, Y. Jia, G. Zhou, X. Li and Y. Zhang, “Low-temperature deposition of ultrafine rutile TiO₂ thin films by the hydrothermal method,” *Physica Status Solidi A*, vol.156, no.2, pp.381-385, 1996.
- [9] X. Yang, C. Cao, L. Erickson, K. Hohn, R. Maghirang and K. Klabunde, “Photo-catalytic degradation of Rhodamine B on C-, S-, N-, and Fe-doped TiO₂ under visible-light irradiation,” *Applied Catalysis B: Environmental*, vol. 91, no.3-4, pp.657-662, 2009.
- [10] R. S. Dubey, and S. Singh, “Investigation of structural and optical properties of pure and chromium doped TiO₂ nanoparticles prepared by solvothermal method,” *Results in Physics*, vol. 7, pp.1283-1288, 2017.
- [11] R. Dholam, M. N. Patel, Adami, and A. Miotello, “Hydrogen production by photocatalytic water-splitting using Cr-or Fe-doped TiO₂ composite thin films photocatalyst,” *International Journal of Hydrogen Energy*, vol.34, no.13, pp.5337-5346, 2009.
- [12] T. Touam, L. Znaidi, D. Vrel, I. Ninova-Kuznetsova, O. Brinza, A. Fischer and A. Boudrioua, “Low Loss Sol-Gel TiO₂ Thin Films for Waveguiding Applications,” *Coatings*, vol.3, no.1, pp.49-58, 2013.
- [13] M. Kitano, R. Mitsui, D. R. Eddy, Z. M. A. El-Bahy, M. Matsuoka, M. Ueshima, and M. Anpo, “Synthesis of Nanowire TiO₂ Thin Films by Hydrothermal Treatment and their Photoelectrochemical Properties,” *Catalysis letters*, vol.119, no. 3-4, pp.217-221, 2007.
- [14] L. Wan, Y. Gao, X. H. Xia, Q. R. Deng and G. Shao, “Phase selection and visible light photo-catalytic activity of Fe-doped TiO₂ prepared by the hydrothermal method,” *Materials Research Bulletin*, vol.46, no.3, pp. 442-446, 2011.
- [15] Y. Xie, L. Wei, G. Wei, Q. Li, D. Wang, Y. Chen, S. Yan, G. Liu, L. Mei and J. Jiao, “A self-powered UV photodetector based on TiO₂ nanorod arrays,” *Nanoscale Research Letters*, vol.8, no.1, pp. 188, 2013.
- [16] T. Theivasanthi and M. Alagar. "Titanium dioxide (TiO₂) nanoparticles XRD analyses: an insight," arXiv preprint arXiv, vol. 1307, pp.1091, 2013.
- [17] S. Manu and M. Abdul Khader, “Non-uniform distribution of dopant iron ions in TiO₂ nanocrystals probed by X-ray diffraction, Raman scattering, photoluminescence and photo catalysis.” *Journal of Materials Chemistry C*, vol.3, no.8, pp.1846-1853, 2015.
- [18] B. Liu and E. S. Aydil, “Growth of Oriented Single-Crystalline Rutile TiO₂ Nanorods on Transparent Conducting Substrates for Dye-Sensitized Solar Cells,” *Journal of the American Chemical Society*, vol.131, no.11, pp. 3985-3990, 2009.